Chemical Geology, 54 (1986) 135—148
Elsevier Science Publishers B.V., Amsterdam — Printed in The Netherlands

STRATIGRAPHIC CONTROL OF RARE-EARTH PATTERN TYPES IN MID-PROTEROZOIC SEDIMENTS OF THE BELT SUPERGROUP, MONTANA, U.S.A.: IMPLICATIONS FOR BASIN ANALYSIS

JUERGEN SCHIEBER

Department of Geology, University of Oregon, Eugene, OR 97403 (U.S.A.)

(Accepted for publication June 18, 1985)

Abstract

Schieber, J., 1986. Stratigraphic control of rare-earth pattern types in Mid-Proterozoic sediments of the Belt Supergroup, Montana, U.S.A.: Implications for basin analysis. Chem. Geol., 54: 135—148.

Within sediments of the Helena embayment, an eastern extension of the Mid-Proterozoic Belt basin, Montana, U.S.A., three different types of REE patterns were identified. The lower part of the investigated sequence (Chamberlain Shale and Lower Newland Formation) is a uniform shale interval which accumulated during a period of tectonic quiescence. The REE patterns of these shales (normalized to NASC) are either flat or LREE enriched, lacking Eu deficiencies. The superjacent unit (Newland Transition Zone) contains variable amounts of feldspathic sandstone. It indicates rejuvenation of the hinterland and regression. The uppermost unit (Upper Newland Formation) consists of alternating packages of carbonates and shales. REE patterns in shales of the Newland Transition Zone and Upper Newland Formation have negative Eu anomalies. This drastic change of REE patterns was observed in all stratigraphic sections.

The source rocks of the Beltian sequence were probably dominated by granitoid gneisses and migmatites, and rocks of this composition show negative Eu anomalies (against NASC) in many other places. The observed negative Eu anomalies in the shales were probably inherited from the source rocks. However, the patterns of the Chamberlain Shale and the Lower Newland Formation are not as easy to explain, because the source rocks seem not to have changed during deposition of the Beltian sequence. Perhaps more intense chemical weathering during Chamberlain Shale—Lower Newland time obscured the negative Eu anomalies in the residual clays. Adsorption of LREE's on clays during transport may have caused the LREE-enriched patterns.

A change in tectonic regime and weathering intensity coincides with the stratigraphic distribution of the different REE pattern types. Thus, stratigraphically controlled REE pattern distribution in a sedimentary basin may help to establish quasi time lines, and may allow monitoring of tectonic pulses and of weathering conditions in the hinterland.

1. Introduction

Geochemists commonly assume that very uniform rare-earth element (REE) patterns develop during formation of sedimentary rocks that may be derived from a diversity of source rocks (e.g., Nance and Taylor, 1976). Since Archean times relative abun-

0009-2541/86/$03.50

dances of REE's in shales have not changed markedly (Wildeman and Haskin, 1973; Nance and Taylor, 1976, 1977) and the vast majority of shales exhibit flat REE patterns when normalized to the North American Shale Composite (NASC). The uniformity of REE patterns in sediments, independent of geography and lithology, is taken as an indication of very effective mixing of clastic components in the sedimentary cycle (Nance and Taylor, 1976). REE patterns in sediments are assumed to reflect the exposed crustal abundances in the source area (McLennan et al., 1980), and variations in REE patterns of a sedimentary province are usually interpreted to reflect differences in source material (Wildeman and Haskin, 1973; Dypvik and Brunfelt, 1976).

This paper reports REE data and selected major- and trace-element data from the Mid-Proterozoic Belt Supergroup, Montana, U.S.A., to show that weathering conditions as well as conditions of deposition have influenced the REE patterns of the shales, and that weathering-related changes of REE patterns allow correlation of stratigraphic sections.

2. Geologic setting

The study area is located in the Little Belt Mountains, Montana (Fig. 1). The shales under study belong to the Neihart Quartzite, Chamberlain Shale and Newland Formation (Walcott, 1899). These sediments were deposited in an eastern extension of the Proterozoic Belt basin, the Helena embayment. Outcrop areas of Proterozoic (Beltian) sediments in the Little Belt Mountains are shown in Fig. 2. Stratigraphic and sedimentologic features of the Beltian sediments in the Helena embayment were investigated by Schieber (1985), and stratigraphic columns and correlations are shown in Fig. 3. Locations of stratigraphic sections are indicated in Fig. 2.

2.1. Stratigraphic features

The basal unit of the Beltian sequence is

Fig. 1. Location map showing outline of Belt basin in the U.S.A. and Canada (*stippled pattern*). *Black rectangle* that is pointed out by *arrow* indicates location of study area.

the Neihart Quartzite, which overlies unconformably the crystalline granitoid basement. The Neihart Quartzite is only exposed in the northern Little Belt Mountains in undisturbed contact with overlying stratigraphic units. In the southern Little Belt Mountains the base of the Beltian sequence is not exposed, and small exposures of the Neihart Quartzite are only found along the Volcano Valley thrust fault (Fig. 2). This lack of exposure as well as lateral facies changes from north to south have in the past hampered correlations between the northern and the southern Little Belt Mountains. For example, Chamberlain Shale lithologies are found only in small exposures in the southern Little Belt Mountains, and the Newland Formation changes its lithologic character towards the south. In the southern Little Belt Mountains the Newland Formation is subdivided into the Upper Newland Formation (intercalated packages of limestone, dolostone and shale) and the Lower Newland Formation (dolomitic shale), whereas in the northern Little Belt Mountains the Newland Formation consists of intercalated packages of dolostone and shale that are lithologically quite different from those

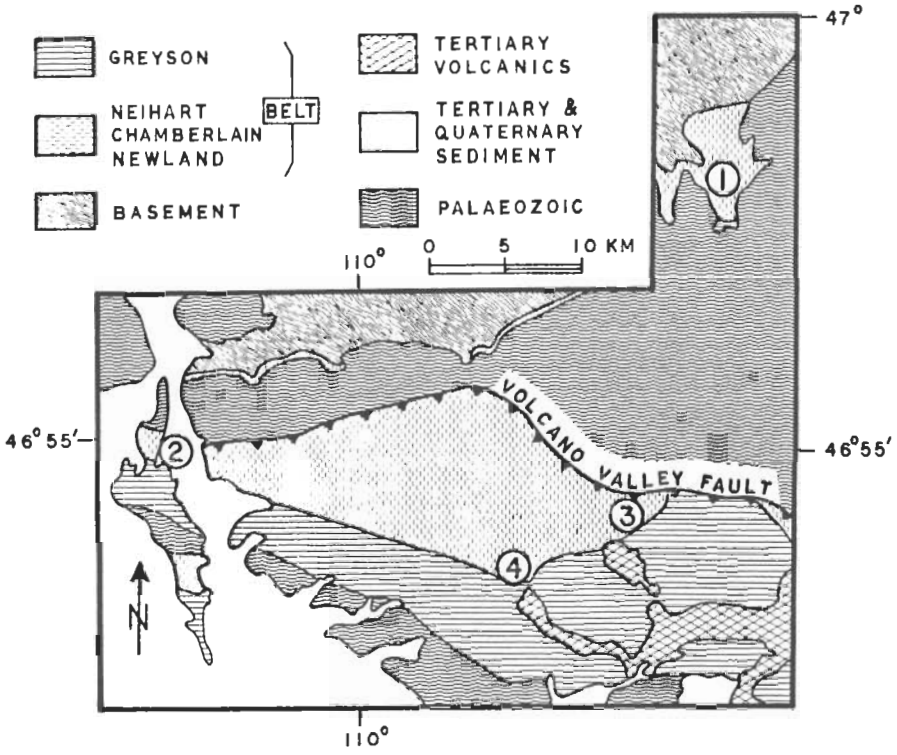

Fig. 2. Geologic overview map of the study area (simplified after McClernan, 1980). The locations of stratigraphic sections that are shown in Fig. 3 are indicated by *circles* with the *section number*. *Teeth* on the trace of the Volcano Valley fault are on the upthrown block.

in the south and cannot be subdivided into an upper and lower member. Stratigraphic subdivisions in the northern Little Belt Mountains are according to Walcott (1899) and those in the southern Little Belt Mountains follow the stratigraphic scheme of Nelson (1963) for the Beltian sequence of the Big Belt Mountains.

In recent work (Schieber, 1985) a distinct horizon with feldspathic sandstones was recognized in the upper one-third of the Chamberlain Shale of the northern Little Belt Mountains, and was found again in stratigraphic sections of the southern Little Belt Mountains. This marker unit is found between the Lower and Upper Newland Formation of the southern Little Belt Mountains, and is provisionally called the Newland Transition Zone in this paper. The Newland Transition Zone is the only unit with feldspathic sandstones in the lower Beltian sequence of the study area, and is one of the backbones of the stratigraphic scheme established by Schieber (1985). Another major correlation unit is the Greyson Formation (Walcott, 1899) which overlies the Newland Formation in both the northern and the southern Little Belt Mountains (Walcott, 1899; Phelps, 1969; Keefer, 1972). These correlations are shown in Fig. 3 and imply that the lower two-thirds of the Chamberlain Shale are lateral equivalents of the Lower Newland Formation, and that the upper one-third of the Chamberlain Shale and the Newland Formation of the northern Little Belt Mountains are lateral equivalents of the Upper Newland Formation of the southern Little Belt Mountains.

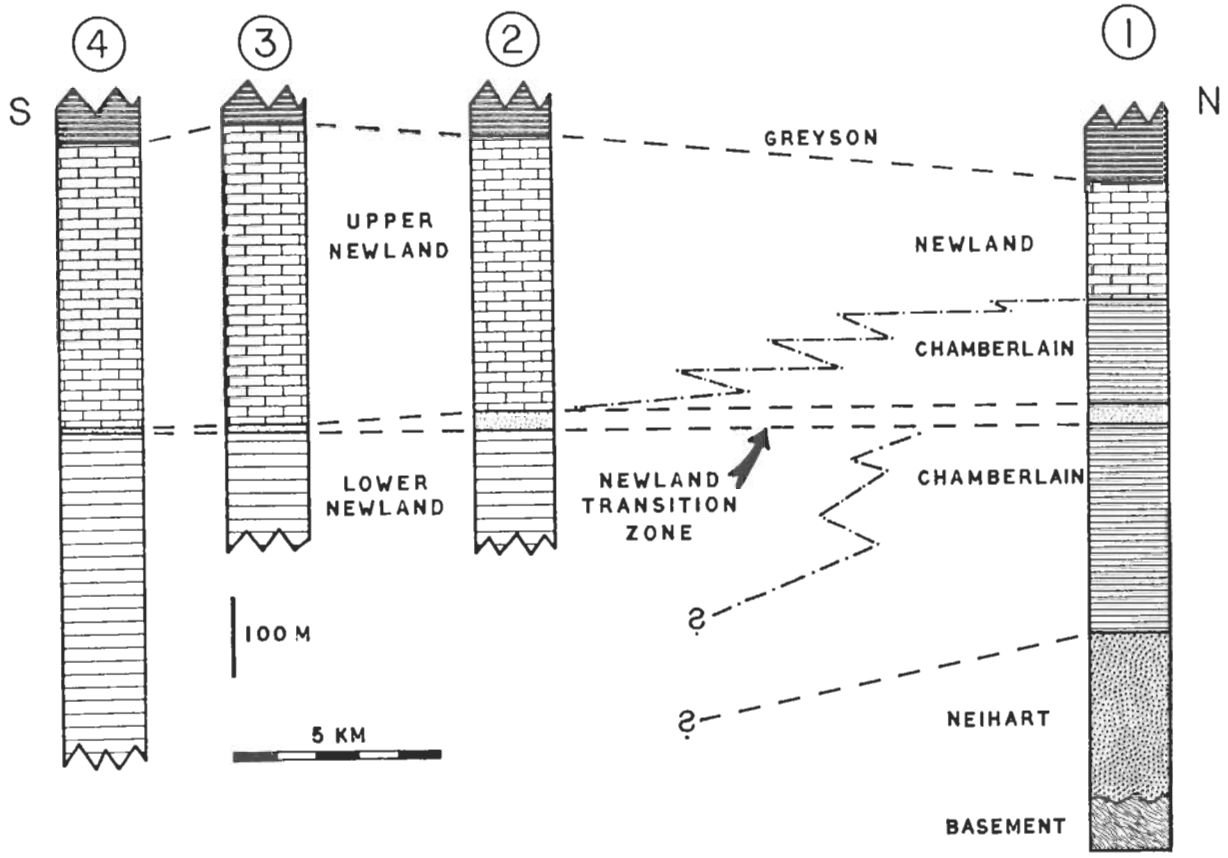

Fig. 3. Simplified stratigraphic sections of the Beltian sequence in the Little Belt Mountains. Only the major stratigraphic units are shown. Stratigraphic sections may have faulted portions. In those cases thicknesses from nearby undisturbed partial sections were used for thickness determinations. Note the lateral equivalency between Chamberlain Shale, Lower Newland Formation and Upper Newland Formation.

2.2. Basin evolution

The evolution of the Helena embayment has recently been described (Schieber, 1985) and will therefore only be briefly discussed here. Deposition of the Belt Supergroup in the Helena embayment commenced with the deposition of the Neihart Quartzite, an orthoquartzite blanket that marks the initial transgression of the Beltian sea. The lower portion of the Neihart Quartzite consists of coarse sandstones with tabular and trough cross-stratification, intercalated lenses of quartz pebbles, and is probably a braided stream deposit. The upper portion of the Neihart Quartzite is finer grained and contains increasing amounts of interbedded shale. Sandstone beds contain mud cracks, wave ripples, beach cross-stratification and mud-chip conglomerates. Shale-rich units show lenticular and wavy bedding. This upper portion of the Neihart Quartzite was probably deposited in a near-shore setting with lagoons, mud flats and beaches. With continuing transgression the Chamberlain Shales were deposited on top of the Neihart Quartzite. These shales exhibit no signs of emergence and were deposited in an offshore setting, while further inside the basin the dolomitic shales of the Lower Newland Formation were deposited. During deposition of the Chamberlain Shale and the Lower Newland Formation a smooth

sediment-filled depression formed in the area of the present-day Helena embayment. The strong predominance of shale deposition, a lack of sandstones, and the generally very uniform appearance of this part of the sequence suggest a hinterland of small relief and tectonic quiescence during deposition of the Chamberlain Shale and the Lower Newland Formation.

Deposition of the Newland Transition Zone marks a major regression. The most conspicuous lithologies are very coarse feldspathic sandstones in erosional channels and lenses of quartz pebble conglomerates. The sandstones are interbedded with shales, may contain mud-chips, and may have mud cracks on bedding planes. The amount of sandstone in the Newland Transition Zone decreases basinwards (towards the south). This pulse of coarse immature sediments is considered to be the result of a major rejuvenation of the hinterland. Increased sedimentation rates caused shallowing and fill-up of marginal portions of the basin, and the basinwards migration of coarse sediment facies. The basin configuration changes to an east—west-trending half-graben during deposition of the Newland Transition Zone, with an active growth fault along the southern margin.

After deposition of the Newland Transition Zone transgression occurs in the north of the basin, whereas the southern basin margin is fixed by the basin-bounding growth fault. Repeated uplifts (of lesser magnitude than that which caused deposition of the Newland Transition Zone) during deposition of the Upper Newland Formation caused cyclic deposition of shales and carbonates.

Several types of shale facies have been distinguished within the sequence under study, and each type can be placed relative to basin margin and center. The first shale type (silty shale) was deposited most marginally in a near-shore environment with intermittent exposure (contains lenticular bedding and mud cracks). The second shale type (algal swirl shale) contains ripped-up fragments of microbial mats and was deposited in a very shallow subaqueous environment with frequent agitation. Basinward of that type comes the striped shale, which consists of interbedded dark carbonaceous shales (probably microbial mat deposits) and gray silt—mud layers that were deposited by storms. The fourth shale type (gray dolomitic shale) was deposited in the central portions of the basin, and shows evidence of reworking by storms.

3. Mineralogic composition of shales

Several hundred petrographic thin sections of shale samples were examined for mineral constituents. Clay mineral compositions of shales were determined by X-ray diffraction.

The shales of the Beltian sequence consist essentially of illite, dolomite, quartz silt, minor amounts of mica flakes (muscovite ± biotite) and detrital feldspar (mainly K-feldspar), and contain trace amounts of heavy minerals (zircon, tourmaline).

Detrital feldspar and biotite are essentially absent in shale samples that were collected below the Newland Transition Zone, but are recognized in the samples from the Upper Newland Formation and especially in those from the Newland Transition Zone. In relative terms the shales of the Newland Transition Zone contain the greatest, and those of the Lower Newland Formation, the Neihart Quartzite and Chamberlain Shale (the lower two-thirds) contain the smallest amount of detrital feldspar and biotite.

4. Sampling and analytical techniques

The shale samples were collected during measurement of the stratigraphic sections shown in Fig. 3. Sampling location and stratigraphic position of each shale sample were recorded. Weathered portions of shale samples were trimmed off, and the remaining sample material was crushed and then ground in a ceramic shatterbox. REE's (La, Ce, Sm, Eu, Tb, Yb and Lu), and Hf, Cr, Co and Th

were determined by instrumental neutron activation analysis. Al_2O_3, K_2O, TiO_2, Zr and Ni were determined by X-ray fluorescence.

5. Results

Of the 41 analyses reported in Table I, 13 are from below the Newland Transition Zone, 11 are from the Newland Transition Zone, and 17 are from the Upper Newland Formation.

There are essentially three different types of NASC-normalized REE patterns that can be recognized. The first type is essentially flat, the second type is ramp shaped because of light rare-earth element (LREE) enrichment, and the third type has negative Eu anomalies. The distribution of REE patterns by stratigraphic unit and shale facies type is shown in Fig. 4. La/Th ratios from the majority of the analyzed shales range from 2 to 4, and the Hf contents of non-dolomitic shale samples range from 3 to 7 ppm. Cr contents in non-dolomitic shales range from several tens to ~100 ppm, Co contents range from 2 to 13 ppm, and Ni contents range from 25 to 70 ppm.

Bhatia and Taylor (1981) and Condie and Martell (1983) point out that sediments derived from granitic crust have small La/Th ratios (1.5—3.5) and large Hf contents (4.5—10 ppm), whereas sediments derived from mafic source rocks have large La/Th ratios (4.5—10) and small Hf contents (0—3.5 ppm). The small La/Th ratios and large Hf contents of the Beltian shale samples indicate therefore that these sediments were derived from a crust of granitic composition. The relatively small contents of Cr, Co and Ni in these shales are further indication that they were derived from a source area of largely granitic composition (Shiraki, 1978; Turekian, 1978a,1978b).

6. Discussion and interpretation of data

The fact that three different types of REE patterns can be recognized in the shales of the Beltian sequence of the Helena embayment raises the question of the significance of this observation, particularly if one notes that most shales from other sedimentary sequences exhibit flat REE patterns when normalized to NASC.

Initially one might think that the different types of patterns are related to different types of shale facies, and may be related to the depositional environment. That, however, is not the case. Fig. 4 shows that a given shale facies type can display each of the three observed pattern types, but the REE pattern type that is characterized by negative Eu anomalies is found only in the Newland Transition Zone and Upper Newland Formation. LREE-enriched and flat patterns can be found throughout the sequence, but they are of minor importance above the Newland Transition Zone. Thus there appears to be stratigraphic control on the distribution of REE pattern types.

REE patterns in sediments usually reflect exposed crustal abundances in their source areas (McLennan et al., 1980). Thus, the change in REE patterns might be explained as a change of source rock owing to uplift. Yet there is reason to believe that the source rock of Beltian sediments were the same below and above the Newland Transition Zone. Pre-Beltian rocks underlying Belt sediments in the Little Belt Mountains consist of granitoid gneisses, migmatites, and some schists. South of the Helena embayment, Precambrian basement rocks in the Tobacco Root Mountains, Highland Mountains, the Ruby Range, and Absaroka Range, and Beartooth Mountains are in general of granitic composition (Wooden et al., 1982; Mueller et al., 1982), similar to those in the Little Belt Mountains. Considerable thicknesses of these deep crustal metamorphic rocks are exposed, but drastic compositional changes with depth are not known to exist. Therefore it seems unlikely that Proterozoic uplift in the Beltian hinterland produced a drastic change in source-rock composition.

An examination of the relationships between Al_2O_3, K_2O and TiO_2 (Fig. 5A and B) for the shale samples that were analyzed in

TABLE I

Analytical data

Sample No.	N1	N2	N3	N4	N5	N6	N7	N8	N9	N10	N11	N12	N13	N14
Stratigraphic unit*[1]	T	T	T	U	U	U	L	L	L	L	L	L	L	U
Shale type*[2]	ST	ST	ST	DS	DS	DS	DS	DS	DS	DS	DS	DS	DS	AS
La (ppm)	46.5	29.9	96.4	12.4	21.1	23.1	26.6	31.5	21.0	21.4	23.3	29.7	17.4	27.0
Ce (ppm)	105	65	211	28	46	48	58	63	44	44	49	60	36	53
Sm (ppm)	7.7	5.5	17.9	2.6	3.4	4.2	4.2	4.5	3.7	4.0	3.6	5.0	3.3	3.9
Eu (ppm)	0.73	1.0	1.33	0.41	0.61	0.67	0.58	0.72	0.58	0.57	0.53	0.73	0.5	0.68
Tb (ppm)	0.9	0.76	2.4	0.39	0.4	0.46	0.51	0.43	0.35	0.34	0.32	0.48	0.24	0.45
Yb (ppm)	3.65	2.94	7.96	1.05	1.4	1.38	1.34	1.9	1.5	1.49	1.03	1.36	1.01	1.69
Lu (ppm)	0.68	0.46	1.25	0.18	0.21	0.25	0.23	0.29	0.23	0.24	0.22	0.2	0.18	0.31
Al_2O_3 (%)	8.91	14.2	12.62	3.96	7.2	7.8	8.12	10.71	5.96	7.14	10.88	8.82	7.2	12.97
K_2O (%)	2.83	3.06	4.06	1.22	1.82	1.01	1.73	2.87	0.95	1.83	2.81	1.81	1.65	2.55
TiO_2 (%)	0.17	0.61	0.23	0.13	0.25	0.24	0.27	0.36	0.19	0.27	0.33	0.32	0.21	0.45
Zr (ppm)	152	305	240	42	54	126	69	85	50	82	73	88	42	139
Hf (ppm)	4.2	8.3	6.6	1.2	1.5	1.9	1.8	2.1	1.5	2.3	2.1	2.4	1.4	3.9
Cr (ppm)	9	69	9	12	26	25	27	34	15	28	40	28	24	60
Co (ppm)	2.0	9.7	1.2	1.7	7.4	2.8	2.9	7.7	4.0	5.9	6.1	4.6	2.1	7.6
Ni (ppm)	n.d.	41	n.d.	n.d.	29	28	30	28	27	29	33	28	28	39
Th (ppm)	15.5	10.9	30.9	3.4	6.8	6.6	7.2	9.7	6.1	7.2	7.5	7.5	5.3	9.3

Sample No.	N15	N16	N17	N18	N19	N20	N21	N22	N23	N24	N25	N26	N27	N28
Stratigraphic unit*[1]	U	U	U	U	T	T	T	T	L	L	L	L	L	L
Shale type*[2]	AS	AS	AS	AS	AS	AS	AS	AS	AS	SS	SS	SS	SS	SS
La (ppm)	31.2	21.0	12.9	28.7	34.5	18.0	43.9	39.6	38.1	40.3	36.1	19.6	16.6	24.5
Ce (ppm)	57	41	25	64	71	34	96	78	84	96	80	40	34	49
Sm (ppm)	4.2	2.6	2.1	5.0	5.4	2.3	7.6	6.0	6.3	7.0	6.1	4.0	3.2	4.4
Eu (ppm)	0.69	0.38	0.38	0.84	0.96	0.37	1.28	1.0	1.22	1.38	1.12	0.71	0.64	0.70
Tb (ppm)	0.49	0.31	0.32	0.73	0.70	0.33	0.81	0.63	0.9	1.04	0.79	0.47	0.45	0.49
Yb (ppm)	1.75	1.41	0.85	2.17	1.82	0.86	2.93	2.25	3.28	3.40	3.58	1.65	1.67	1.73
Lu (ppm)	0.39	0.24	0.14	0.39	0.29	0.15	0.51	0.47	0.46	0.57	0.56	0.28	0.29	0.37
Al_2O_3 (%)	12.77	9.96	4.02	8.4	13.55	8.25	18.13	15.88	16.88	17.32	14.87	6.34	6.25	8.09
K_2O (%)	2.61	2.17	0.57	1.69	4.02	2.19	5.01	4.60	3.20	3.70	2.90	1.49	1.38	1.74
TiO_2 (%)	0.50	0.37	0.14	0.27	0.52	0.29	0.70	0.60	0.64	0.65	0.66	0.31	0.29	0.35
Zr (ppm)	126	107	29	89	85	60	124	117	131	177	246	95	107	112
Hf (ppm)	3.2	3.2	0.9	2.4	3.0	1.6	3.1	3.0	3.5	3.4	6.5	2.4	2.6	3.3
Cr (ppm)	56	40	16	19	70	41	107	85	93	88	83	27	24	31
Co (ppm)	6.7	5.1	3.3	4.5	8.3	5.8	9.4	7.4	25.2	8.4	8.1	5.9	6.6	6.2
Ni (ppm)	36	28	n.d.	26	45	35	50	42	58	67	48	25	32	35
Th (ppm)	11.2	8.2	3.0	8.9	8.3	5.1	13.0	10.9	11.2	10.8	11.2	6.6	6.2	7.9

Sample No.	N29	N30	N31	N32	N33	N34	N35	N36	N37	N38	N39	N40	N41
Stratigraphic unit*[1]	U	U	U	U	U	U	U	U	U	T	T	T	T
Shale type*[2]	SS	SS	SS	SS	SS	SS	SS	SS	SS	SS	SS	SS	SS
La (ppm)	33.4	17.9	19.3	16.0	32.7	12.7	17.7	23.7	24.0	16.1	21.3	19.2	22.4
Ce (ppm)	75	38	40	34	69	25	37	46	50	35	42	39	52
Sm (ppm)	7.2	3.7	3.2	3.0	5.7	2.3	2.9	3.9	4.2	2.9	3.4	3.1	5.6
Eu (ppm)	0.69	0.62	0.58	0.36	0.88	0.34	0.66	0.54	0.51	0.49	0.58	0.53	0.85
Tb (ppm)	1.06	0.42	0.48	0.35	0.75	0.22	0.42	0.59	0.57	0.30	0.46	0.43	0.78
Yb (ppm)	4.38	1.84	1.25	1.62	3.18	1.14	1.15	1.92	2.08	0.98	1.54	1.45	2.14
Lu (ppm)	0.59	0.25	0.21	0.25	0.75	0.22	0.17	0.28	0.41	0.19	0.26	0.25	0.40
Al_2O_3 (%)	11.26	10.94	6.08	8.52	12.60	6.17	5.10	8.74	8.83	6.23	7.70	5.07	6.97
K_2O (%)	3.64	3.54	0.88	1.59	2.58	1.27	0.58	1.71	2.22	1.16	2.15	1.20	1.14
TiO_2 (%)	0.37	0.31	0.20	0.33	0.56	0.27	0.15	0.30	0.33	0.19	0.27	0.25	0.28
Zr (ppm)	184	147	62	99	214	85	53	88	142	48	137	102	98
Hf (ppm)	5.5	3.8	1.6	1.7	6.0	2.2	1.4	2.6	2.8	1.3	3.4	2.5	2.9
Cr (ppm)	27	26	21	28	47	30	18	31	29	20	27	23	28
Co (ppm)	4.8	7.4	3.2	4.3	5.1	13.8	2.0	2.7	6.4	3.9	4.7	5.6	12.1
Ni (ppm)	29	28	26	29	31	64	n.d.	n.d.	38	26	32	26	31
Th (ppm)	14.5	7.1	4.6	6.7	10.5	4.8	3.9	6.5	9.7	5.6	8.2	5.4	6.9

*[1] L = Lower Newland Formation and equivalents; T = Newland Transition Zone; U = Upper Newland Formation and equivalents.
*[2] AS = algal swirl shale; DS = gray dolomitic shale; SS = striped shale; ST = silty shale.

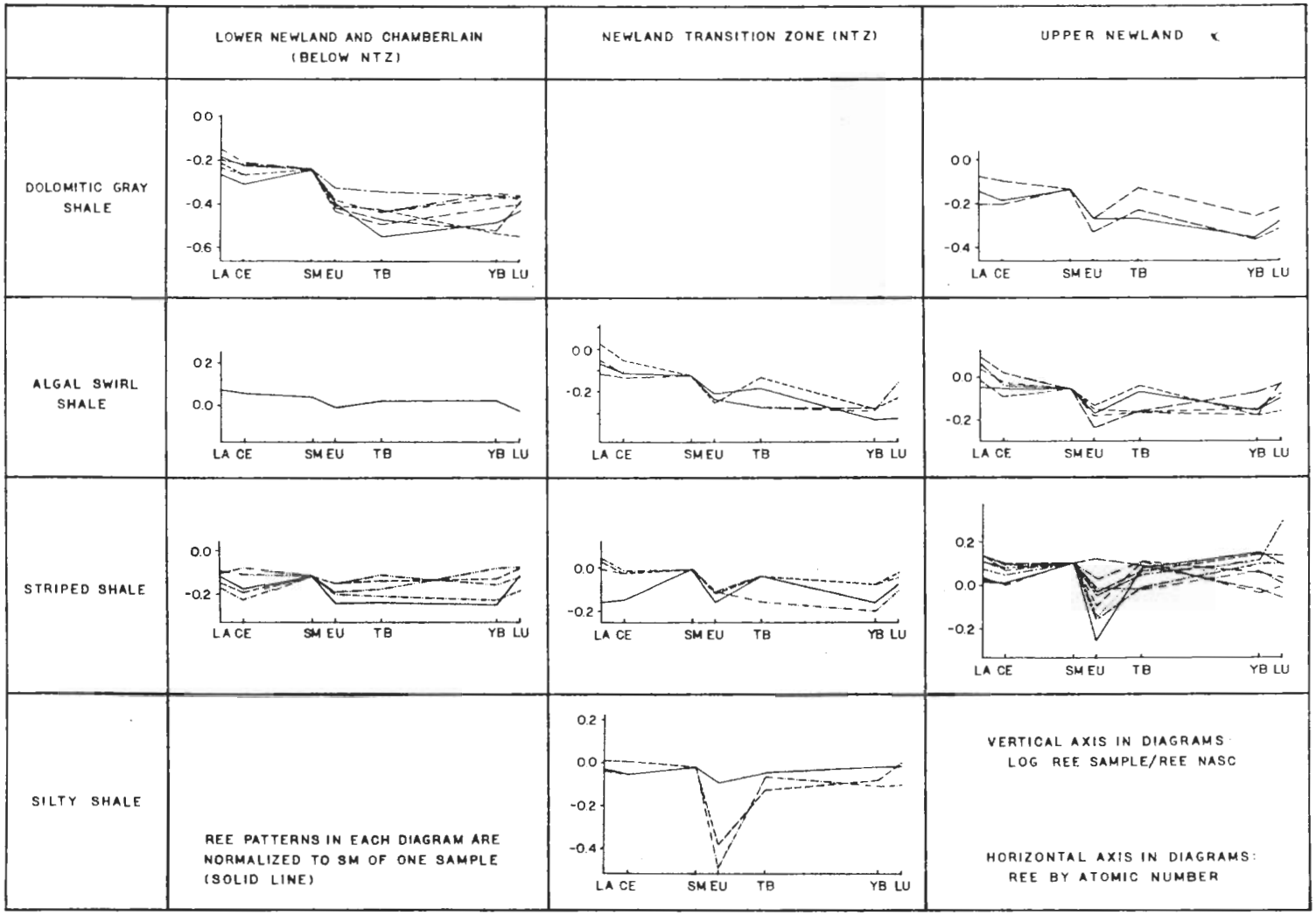

Fig. 4. Distribution of REE pattern types by stratigraphic subdivision and shale type in the Beltian shales of this study.

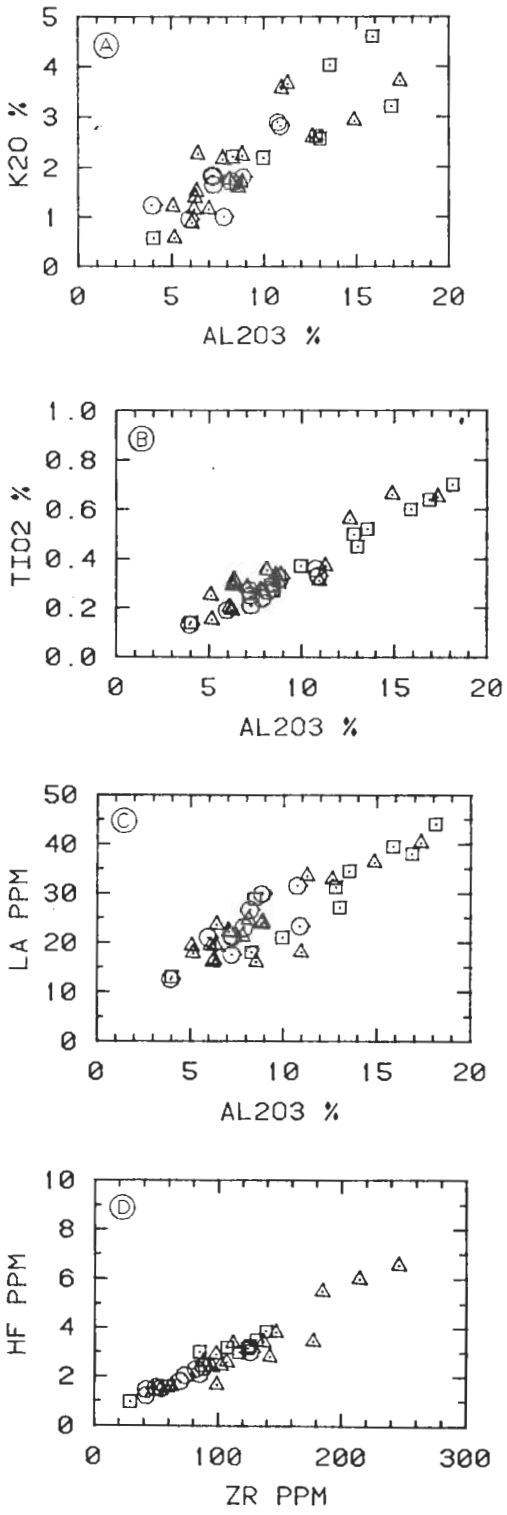

this study demonstrate a remarkably uniform composition of the Beltian sequence. The correlation between Al_2O_3 and K_2O in Fig. 5A indicates that most of the K of the samples is contained in the clays. The diagram also indicates that detrital feldspars that were observed in the shales make no significant contribution to the K content of the shales, otherwise the shales from the Newland Transition Zone should show significantly smaller Al_2O_3/K_2O ratios than do the other shale samples. The scatter of data points in Fig. 5A is probably caused by variations in the detrital feldspar content of the samples. The correlation between Al_2O_3 and TiO_2 indicates that practically all Ti is contained in the clay minerals. The data points in Fig. 5A and B are from the whole thickness of the Beltian sequence under discussion here. The clays constitute practically the entire terrigenous contribution to the chemical composition of these shales. The fact that the clays of this sequence are of very uniform composition throughout a considerable stratigraphic thickness indicates that the source rocks were of fairly similar composition throughout. The small La/Th ratios and large Hf contents of all the shale samples (see Section 5) are in support of this assumption and together with the relatively small Cr, Co and Ni contents they also indicate a granitoid source terrane.

Obradovich and Peterman (1968) determined Rb–Sr ages for argillaceous samples of the Beltian sequence in the Big Belt Mountains and little Belt Mountains. Samples for the sequence from Neihart Quartzite to Greyson Formation form a good isochron, and have essentially the same initial $^{87}Sr/^{86}Sr$ ratios. This result may indicate that the clays of these samples were derived from the same type of source rock.

The terrigenous detrital fraction of the

Fig. 5. Relationship between : (A) K_2O and Al_2O_3; (B) TiO_2 and Al_2O_3; (C) La and Al_2O_3; and (D) Zr and Hf, in Beltian shales (*circles* = samples of gray dolomitic shale; *triangles* = striped shale samples; *squares* = samples of algal swirl shale).

shales (predominantly clay) contains essentially all of the REE in the shales (good correlation between REE and Al_2O_3 in Fig. 5C), and because a change of source rock is not a very likely cause of the change in REE patterns, another possible explanation for the variable REE patterns is that they were influenced by weathering conditions, and that the latter underwent some changes.

6.1. Possible causes for negative Eu anomalies

The source rocks for Beltian sedimentation likely consisted of granitoid gneisses and migmatites. NASC-normalized patterns of gneisses (data from McCarthy and Kable, 1978) may show weak negative Eu anomalies. Eu anomalies (normalized against NASC) become quite pronounced when REE patterns of migmatites (data from McCarthy and Kable, 1978) are examined. Proterozoic granites from New Mexico which are thought to have originated by partial melting (Condie, 1978), also show clear negative Eu anomalies in REE patterns when normalized to NASC. Emmermann et al. (1975) observed an increase in magnitude of negative Eu anomalies and a parallel increase in total REE during progressive anatexis of gneisses in the Black Forest, southwest Germany. They explained the phenomenon with incongruent melting of biotites. The biotites are the major REE carriers in these gneisses and exhibit a strong negative Eu anomaly. With increased melting more and more biotite will go into the melt, raise its total REE content, and will also cause an increasingly stronger Eu anomaly in the melt. The granites which result from such partial melts have larger total REE contents and negative Eu anomalies. Emmermann et al. (1975) normalized the REE's of the Black Forest granites against chondrites (where they showed negative Eu anomalies), but the negative Eu anomalies of these granites are still clearly visible when their REE contents are normalized against NASC. The above discussion shows that granitoid gneisses and migmatites can be expected to have negative Eu anomalies when normalized against NASC. It is therefore likely that the metamorphic source terrane of the Belt series has an overall negative Eu anomaly when normalized against NASC. If REE patterns in sediments are characteristic of exposed crustal abundances (McLennan et al., 1980), then we might expect that the sediments derived from the metamorphic source terrane of the Belt series inherited a negative Eu anomaly.

This anomaly is in fact clearly visible in the rocks of the Newland Transition Zone and Upper Newland Formation, but not in sediments of the Lower Newland Formation and its lateral equivalent, the Chamberlain Shale.

6.2. Influence of weathering on REE *patterns*

Behaviour of REE during weathering of a granodiorite has been investigated by Nesbitt (1979), who found that residual clays are depleted in heavy REE's (HREE's) relative to the parent rock and also have smaller total REE abundances. In contrast the altered parent rock was enriched in HREE's and had larger total REE abundances than did the parent rock. Nesbitt noted that mixing of weathering products would produce a REE pattern similar to those of the fresh granodiorite and NASC, and also that size sorting of weathering products during sediment transport might produce sediments with fractionated REE patterns (shales with HREE depletion and sandstones with HREE enrichment). In Nesbitt's example the low pH in the topsoil (caused by decay of organic matter) promotes leaching of REE's from the residual clays, and because plant cover was absent in the Precambrian, the described fractionation process may not have been very effective in the Precambrian. Cullers et al. (1975), from a study of clays in shales, suggest that intense weathering may decrease total REE's in clays, and also may decrease the LREE/HREE ratio. They also found negative Eu anomalies (vs. NASC) in clays, which were interpreted as inherited from the source rock, rather than from selective Eu leaching during weathering.

Dypvik and Brunfelt (1976), in a study of REE's in lower Paleozoic shelf sediments of Norway, conclude that faster sedimentation and less intense weathering leads to REE patterns that reflect the source rock to a certain extent, and that slow sedimentation (usually concomitant with a hinterland of muted relief and predominance of chemical weathering) gives better mixing possibilities for sediment from different source areas. They assume that stronger chemical weathering will favour REE fractionation (greater LREE/HREE ratios). It is also noted by Dypvik and Brunfelt (1976) that greater LREE/HREE ratios can be caused by selective adsorbtion of LREE's on clays in seawater (a process favoured by slow deposition and reworking).

6.3. *Interpretation of* REE *patterns in the Beltian Shales*

With this information one can attempt to interpret the REE patterns encountered in the shales of the Newland Formation. The LREE-enriched patterns of the shales of the Lower Newland Formation might for example indicate fractionation in the source area, in the same way as suggested by Nesbitt (1979). However, from Fig. 4 one can see that the REE patterns from the Lower Newland—Chamberlain sequence with the strongest relative LREE enrichment are found in the gray dolomitic shale facies, which was deposited in the central portions of the basin. Thus it appears that the length of the transport path of the clays has an influence on the LREE enrichment of the shales.

Variations in the heavy-mineral content of a shale might also have an influence on the LREE/HREE ratio of a shale sample. Heavy minerals can contribute noticeable amounts of REE's to shales, and variations in heavy-mineral concentrations may account for some of the scatter in Fig. 5C. In a recent investigation of the NASC (Gromet et al., 1984) it was found that heavy minerals contain about one-third of the HREE's in the NASC. Therefore, apparent LREE enrichment of a shale sample could also be brought about by a depletion of heavy minerals in the sample.

The most abundant heavy mineral in the Beltian shales under study is zircon, and the good correlation between Zr and Hf (Fig. 5D) shows that essentially all the Zr in the samples is contained in detrital zircon. If zircon content were to have an influence on the LREE/HREE ratio of these shales, then the samples of silty shale which have considerably larger Zr/Al_2O_3 ratios ($17 \cdot 10^{-4}$—$26 \cdot 10^{-4}$) than those of other shale samples in the sequence ($7 \cdot 10^{-4}$—$17 \cdot 10^{-4}$), should show HREE enrichment relative to other shales of the sequence. However, this is not the case, and therefore we may assume that HREE contribution by heavy minerals has no significant impact on the patterns of the shales under study. The REE content of these shales probably predominantly resides in the clays (Fig. 5C).

The contrast in LREE enrichment between basin center and basin margin may indicate adsorption of REE's on clays during transport into the basin (Dypvik and Brunfelt, 1976). LREE's would be preferred in this process, because of the smaller stability of LREE aqueous complexes. Adsorption of REE's on clays with concomitant REE fractionation is

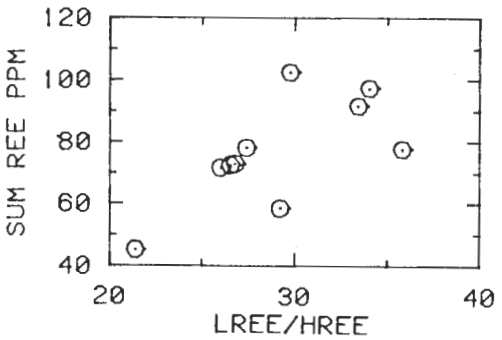

Fig. 6. Relationship between the sum of REE and the LREE/HREE ratio in gray dolomitic shales. Because the LREE's La and Ce have large relative abundances in shales, LREE enrichment would cause considerable increases in the La and Ce content of shale samples and would lead to substantial increases of the total REE content of samples.

indicated by a positive correlation between total REE's and LREE/HREE in the samples of gray dolomitic shale, which have the strongest LREE enrichment (Fig. 6).

6.4. Summary

As outlined above, the observed stratigraphic distribution of REE patterns in shales of the Helena embayment most likely was not caused by a difference in source rock between Chamberlain Shale—Lower Newland Formation and Newland Transition Zone—Upper Newland Formation. The tectonic quiescence and strong dominance of shale during deposition of the Lower Newland Formation and the lower two-thirds of the Chamberlain Shale suggest that the hinterland was of very low relief during that time. The previously noted lack of detrital feldspar in that part of the sequence indicates that chemical weathering went to completion. When rejuvenation of the hinterland occurred at the time of deposition of the Newland Transition Zone, the shales incorporated detrital feldspar and biotite and the associated sandstones contain as much as 15% detrital feldspar. That observation indicates that chemical weathering did not go to completion during that time, and that the hinterland had stronger relief when compared to earlier times. Shale and carbonate deposition was strongly dominant during Upper Newland time, an indication that the relief of the hinterland was reduced when compared to the Newland Transition Zone. However, the presence of detrital feldspar and biotites in the shales indicates that chemical weathering did not go to completion.

More intense chemical weathering (probably related to a hinterland of very muted relief and to tectonic quiescence) may have decreased the total REE content in the residual clays (Cullers et al., 1975), and may have caused obliteration of original negative Eu anomalies in the Chamberlain Shale and the Lower Newland Formation. That intensity of weathering is related to the total REE content of shale samples and to the preservation of the original negative Eu anomaly is supported by the observation that samples with unusually large total REE contents and very strong negative Eu anomalies are found only in the Newland Transition Zone (samples N*1* and N*3*) where the most immature sediments of the sequence are found. One may therefore say that the negative Eu anomalies that were probably present in the gneissic and migmatitic source rocks of the Beltian sequence of the Helena embayment were inherited by the sediments at times of incomplete chemical weathering (probably linked to uplift in the hinterland).

Ramp-like REE patterns in the Beltian shale sequence were probably not caused by stronger chemical weathering (Dypvik and Brunfelt, 1976) or heavy-mineral depletion (Gromet et al., 1984). The observed general increase of LREE enrichment in these shales from basin margin to basin center indicates that the length of the transport path of the clay minerals is of importance for LREE enrichment.

The absence of negative Eu anomalies in some samples from the Newland Transition Zone and the Upper Newland Formation might be explained in various ways. In the case of the Newland Transition Zone the clays of these samples could for example have been derived from remnants of the pre-rejuvenation weathering blanket. During the time of deposition of the Upper Newland Formation more strongly leached weathering blankets may have accumulated during periods of major carbonate deposition. These weathering blankets may have been the source rocks of shale samples without negative Eu anomalies in the Upper Newland Formation. Repeated resuspension during reworking of algal swirl shales may have enhanced LREE enrichment in this shale facies, and may additionally explain ramp-like patterns in algal swirl shales of the Newland Transition Zone and Upper Newland Formation. There is a possibility that negative Eu anomalies in clays might be obliterated by LREE enrichment during transport and deposition of the clays.

7. Conclusion

Four measured stratigraphic sections in the Little Belt Mountains encompass the three major stratigraphic units (Lower Newland Formation—Chamberlain Shale, Newland Transition Zone and Upper Newland Formation) previously discussed. From all four sections, samples from each of these three units were analyzed and showed very clearly the described stratigraphic distribution of REE patterns.

It appears that REE patterns can be used by themselves to draw conclusions about weathering conditions and tectonic regime of the hinterland of a sedimentary basin, and that distribution of REE patterns in sedimentary sequences may be a powerful tool to correlate stratigraphic sections. Correlations of this kind could be considered as approximate time lines, monitoring pulses of uplift in the hinterland.

In most Precambrian basins a lithostratigraphic approach to basin analysis must be taken for the lack of index fossils, and this approach can become quite difficult when shales are the dominant lithology. Detailed studies of such basins show in most cases that lithofacies are diachronous, yet to what degree is difficult to estimate. By determining REE pattern distribution in stratigraphic sections, one might be able to trace changes of tectonic activity from the marginal (often sand dominated) portions of a basin into the central (usually shale dominated) portions (Fig. 7), thus allowing establishment of time equivalency of stratigraphic units. This would in turn lead to a clearer picture of the basin evolution.

Deciphering of tectonic pulses will be easiest, when the source rocks remain the same for long periods of sedimentation, and if there is little variation in source-rock lithology around the sedimentary basin. If source-rock composition is variable through time and space, it will have an impact on the resulting REE patterns, and their interpretation will face increasing difficulties. Therefore, before applying this method, the overall homogeneity of the source area has to be evaluated, either by direct knowledge of the likely source rocks and their mineralogical and chemical composition, or by means of petrographic and geochemical studies of the sediments that give information about the source rocks. Clearly, this method is most suitable for sequences that overlie relatively homogeneous shield areas, yet another reason why it might be most profitably applied to Precambrian basins.

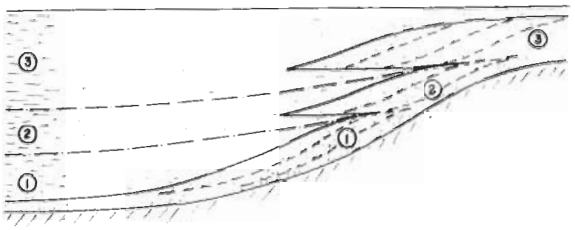

Fig. 7. Hypothetic cross-section of shale-dominated basin. Three successive regressive—transgressive clastic cycles (*index number* of cycle *in circle*) would be recognized in stratigraphic sections along the basin margin (right part of diagram). In the basin center only a uniform shale sequence would be recognized (*numbers in circles* mark shale packages that are lateral equivalents of coarse clastic cycles at the basin margin). With the help of REE pattern changes it might be possible to recognize the base of each new regressive cycle, analogous to the recognition of the Lower Newland—Newland Transition Zone contact in the Belt basin.

Acknowledgements

The author wishes to thank Dr. Gordon Goles for helpful discussions and suggestions that improved the manuscript. Field work and analytical work was supported by Anaconda Minerals Company.

References

Bhatia, M.R. and Taylor, S.R., 1981. Trace element geochemistry and sedimentary provinces: Study from the Tasman geosyncline, Australia. Chem. Geol., 33: 115—125.

Condie, K.C., 1978. Geochemistry of Proterozoic

granitic plutons from New Mexico, U.S.A. Chem. Geol., 21: 131—149.

Condie, K.C. and Martell, C., 1983. Early Proterozoic metasediments from north-central Colorado: Metamorphism, provenance, and tectonic setting. Geol. Soc. Am. Bull., 94: 1215—1224.

Cullers, R.L., Chaudhuri, S., Arnold, B., Moon, L. and Wolf, C.W., 1975. Rare earth distributions in clay minerals and in the clay-sized fraction of the Lower Permian Havensville and Eskridge shales of Kansas and Oklahoma. Geochim. Cosmochim. Acta, 39: 1691—1703.

Dypvik, H. and Brunfelt, A.O., 1976. Rare-earth elements in Lower Paleozoic epicontinental and eugeosynclinal sediments from the Oslo and Trondheim regions. Sedimentology, 23: 363—378.

Emmermann, R., Daieva, L. and Schneider, J., 1975. Petrologic significance of rare earth distribution in granites. Contrib. Mineral. Petrol., 52: 267—283.

Gromet, L.P., Dymek, R.F., Haskin, L.A. and Korotev, R.L., 1984. The "North American shale composite": Its compilation, major and trace element characteristics. Geochim. Cosmochim. Acta, 48: 2469—2482.

Keefer, W.R., 1972. Geologic map of the west half of the Neihart 15-minute quadrangle, central Montana. U.S. Geol. Surv., Misc. Invent. Map I-726 (scale 1 : 62,500, 1 sheet).

McCarthy, T.S. and Kable, E.J.D., 1978. On the behaviour of rare earth elements during partial melting of granitic rock. Chem. Geol., 22: 21—29.

McClernan, H.G., 1980. Metallogenic map of the White Sulfur Springs Quadrangle, Central Montana. Mont. Bur. Min. Geol., Geol. Map 7 (scale 1 : 250,000, 2 sheets).

McLennan, S.M., Nance, W.B. and Taylor, S.R., 1980. Rare earth—thorium correlations in sedimentary rocks, and the composition of the continental crust. Geochim. Cosmochim. Acta, 44: 1833—1839.

Mueller, P.A., Wooden, J.L., Odom, A.L. and Bowes, D.R., 1982. Geochemistry of the Archean rocks of the Quad Creek and Hellroaring Plateau areas of the eastern Beartooth. Mont. Bur. Min. Geol., Spec. Publ., 84: 69—82.

Nance, W.B. and Taylor, S.R., 1976. Rare earth element patterns and crustal evolution, I. Australian post-Archean sedimentary rocks. Geochim. Cosmochim. Acta, 40: 1539—1551.

Nance, W.B. and Taylor, S.R., 1977. Rare earth element patterns and crustal evolution, II. Archean sedimentary rocks from Kalgoorlie, Australia. Geochim. Cosmochim. Acta, 41: 225—231.

Nelson, W.H., 1963. Geology of the Duck Creek Pass quadrangle, Montana. U.S. Geol. Surv., Bull. 1121J, 56 pp.

Nesbitt, W.H., 1979. Mobility and fractionation of rare earth elements during weathering of a granodiorite. Nature (London), 279: 206—210.

Obradovich, J.D. and Peterman, Z.E., 1968. Geochronology of the Belt Series, Montana. Can. J. Earth Sci., 5: 737—747.

Phelps, G.B., 1969. Geology of the Newland Creek area, Meagher Cty., Montana. Master's Thesis, Montana College Mineral Sciences and Technology, Butte, Mont., 56 pp.

Schieber, J., 1985. The relationship between basin evolution and genesis of stratiform sulfide horizons in Mid-Proterozoic sediments of Central Montana (Belt Supergroup). Ph.D. Dissertation, University of Oregon, Eugene, Oreg., 810 pp.

Shiraki, K., 1978. Chromium. In: K.H. Wedepohl (Editor), Handbook of Geochemistry. Springer, Heidelberg, pp. 24-E-1—24-K-7.

Turekian, K.K., 1978a. Cobalt. In: K.H. Wedepohl (Editor), Handbook of Geochemistry. Springer, Heidelberg, pp. 27-E-1—27-K-4.

Turekian, K.K., 1978b. Nickel. In: K.H. Wedepohl (Editor), Handbook of Geochemistry. Springer, Heidelberg, pp. 28-E-1—28-E-4.

Walcott, C.D., 1899. Precambrian fossiliferous formations. Geol. Soc. Am. Bull., 10: 199—244.

Wildeman, T.R. and Haskin, L.A., 1973. Rare earths in Precambrian sediments. Geochim. Cosmochim. Acta, 37: 419—438.

Wooden, J.L., Mueller, P.A., Hunt, D.K. and Bowes, D.R., 1982. Geochemistry and Rb—Sr geochronology of Archean rocks from the interior of the southeastern Beartooth Mountains, Montana and Wyoming. Mont. Bur. Min. Geol., Spec. Publ., 84: 45—56.